Appl. Phys. B 73, 541–545 (2001)
DOI: 10.1007/s003400100717

Applied Physics B
Lasers and Optics

I.F. SALAKHUTDINOV[1,3,✉]
L. KOTAČKA[2,3]
H.J.W.M. HOEKSTRA[3]
J. ČTYROKÝ[2]
V.A. SYCHUGOV[1]
O. PARRIAUX[4]

Abnormal reflecting mirror structures for intra-cavity Čerenkov second-harmonic generation

[1] General Physics Institute, Vavilov str. 38, Moscow 117 942, Russia
[2] Institute of Radio Engineering and Electronics, Prague, The Czech Republic
[3] Department of Applied Physics, MESA+ Research Institute, University of Twente, Enschede, The Netherlands
[4] Laboratoire TSI, Université Jean Monnet, St. Etienne, France

Received: 16 May 2001 /Revised version: 28 August 2001
Published online: 30 October 2001 •

ABSTRACT Abnormal reflecting mirror (ARM) structures, consisting of a corrugated optical waveguiding structure, can serve as a wavelength-selective end mirror in a laser cavity. The ARM structure shows, for each wavelength in a certain region, 100% reflection at a certain angle of incidence. In the vicinity of this angle the waveguide is resonantly excited, leading to strong enhancement of the optical field in the layer structure, which is interesting for efficient second-harmonic generation (SHG). In this paper, experimental results of a first prototype, exhibiting Čerenkov SHG, are reported.

PACS 41.60.Bq; 42.40.Eq; 42.79.Nv; 42.65.Wi; 42.82.E

1 Introduction

Due to the growing importance of coherent short-wavelength sources (green/blue light), efficient sources for second-harmonic generation (SHG) are very attractive. Here one may choose between guided–guided SHG, where guided modes are involved at both frequencies, or the so-called Čerenkov SHG (ČSHG), where the second-harmonic light is radiative [1–6]. The latter is often believed to be less efficient but also less stringent with respect to phase matching, but as was shown by Asai et al. [4] for the first time, the conversion efficiency of ČSHG exhibits a few very sharp maxima as a function of the wavelength and the layer thickness (see also [6]). The origin of this feature was discussed in [5, 6]. It was shown theoretically [6] that more degrees of freedom, with respect to the wavelengths corresponding to such peaks, are introduced by using three- and four-layer systems. It was also shown, both theoretically [4] and experimentally [2, 3], that the peak conversion efficiency is just a transition point between ČSHG and the SHG of a guided mode. A normalised conversion efficiency of about 1000%/W cm^2 was reported [3]. In this work we present theoretical and experimental results of ČSHG in a not yet fully optimised, with respect to SHG, abnormal reflecting mirror (ARM) device.

✉ Fax: +007-095/1350-270, E-mail: ildar@kapella.gpi.ru

2 Čerenkov-regime SHG

This section describes basic properties of the Čerenkov-regime SHG. First of all, only relevant expressions from the theory are extracted and adapted. Furthermore, only the $TE^{\omega} - TE^{2\omega}$ conversion is considered because the results relating to the *TM* modes may be deduced similarly to the corresponding results for the *TE* modes. The conversion of the fundamental TE^{ω} guided mode to the second-harmonic $TE^{2\omega}$ radiation mode is analysed using the coupled-mode analysis in the configuration of a three-layer slab optical waveguide.

A waveguiding high-refractive-index layer of the thickness h made from an optically linear material is deposited onto a non-linear substrate (the only substrate we consider is non-linear; in our case KTP is exploited) and covered by a lower-index superstrate. The axis z belongs to the propagation direction of the fundamental guided mode. The principle of the ČSHG is as depicted in Fig. 1, i.e. the phase matching between the pump guided mode and the generated second-harmonic mode is satisfied automatically [1]. The second-harmonic radiation leaks into the substrate under a pertinent Čerenkov angle, which thus obeys the relation

$$\cos\theta = N_{\omega}/n_{s,2\omega}\,. \tag{1}$$

N_{ω} is the effective index of the fundamental guided mode and $n_{s,2\omega}$ is the refractive index of the substrate for the second-harmonic radiation.

If Tamada's procedure [1] is followed then the distribution of the guided fundamental (ω) field in the substrate, i.e. for $x < -h$, obeys the relation

$$E_{y,\omega} = A_g \left[\cos(\kappa h) + \frac{\delta}{\kappa}\sin(\kappa h)\right] \exp[\gamma(x+h)]\,, \tag{2}$$

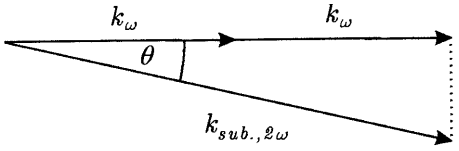

FIGURE 1 The phase-matching diagram in the case of ČSHG

where $\kappa = k\left(n_{\mathrm{g},\omega}^2 - N_\omega^2\right)^{1/2}$, $\gamma = k\left(N_\omega^2 - n_{\mathrm{s},\omega}^2\right)^{1/2}$, and $\delta = k\left(N_\omega^2 - n_{\mathrm{c},\omega}^2\right)^{1/2}$, with $k = 2\pi/\lambda$. The subscripts g, s, and c relate to a guide, a substrate, and a cladding, respectively. The normalisation constant A_g is given by (see for the whole theoretical background e.g. [7, Chapt. 1])

$$A_\mathrm{g} = \left(\frac{4\omega\mu_0\kappa^2}{\beta_\omega(\kappa^2-\delta^2)(h+\gamma^{-1}+\delta^{-1})}\right)^{1/2} \tag{3}$$

to fulfil the condition $\int_{-\infty}^{\infty}|E_{y,\omega}|^2\,\mathrm{d}x = 1$ (W/m). The second-harmonic field is expressed as a radiation mode. Thus,

$$E_{y,2\omega} = A_\mathrm{r}\left\{\left[\cos(\sigma x)+\frac{\Delta}{\sigma}\sin(\sigma x)\right]\cos\left[\varrho(x+h)\right] + \frac{\sigma}{\varrho}\left[\sin(\sigma x)-\frac{\Delta}{\sigma}\sin(\sigma x)\right]\sin\left[\varrho(x+h)\right]\right\} \tag{4}$$

where $\sigma = 2k\left(n_{\mathrm{g},2\omega}^2 - N_\omega^2\right)^{1/2}$, $\varrho = 2k\left(n_{\mathrm{s},2\omega}^2 - N_\omega^2\right)^{1/2}$, and $\delta = 2k\left(N_\omega^2 - n_{\mathrm{c},2\omega}^2\right)^{1/2}$. The normalisation constant A_r is given as follows:

$$A_\mathrm{r} = \left(\frac{8\omega\mu_0\sigma^2\varrho^2}{\pi\beta_\omega\left\{\sigma^2[\sigma\sin(\sigma h)-\Delta\cos(\sigma h)]^2+\varrho^2[\sigma\cos(\sigma h)+\Delta\sin(\sigma h)]^2\right\}}\right)^{1/2}. \tag{5}$$

As the next step the wave equation with a perturbed polarisation vector is to be solved (for details see e.g. [1] or especially [8]). The solution of the wave equation leads to the following expression describing the generated second-harmonic power $P_{2\omega}$ as the function of the pump power P_ω and the interaction length L (we integrate over all radiation modes, because of the continuum of the radiation-mode propagation constants):

$$P_{2\omega} = P_\omega^2 L^2 \int_0^\infty \eta I_\mathrm{pm}\,\mathrm{d}\varrho\,. \tag{6}$$

The quantity η is the so-called normalised conversion efficiency given by

$$\eta = d_{33}^2\omega^2\varepsilon_0^2|F|^2\,, \tag{7}$$

where ω is the frequency of the fundamental radiation, ε_0 is the permittivity of the vacuum, and d_{33} is a pertinent nonlinear coefficient (i.e. d_{33} plays an essential role in the configuration exploiting KTP). The so-called overlap integral F is defined by

$$F = \int_\mathrm{sub.} E_{y,\omega}^2 E_{y,2\omega}\,\mathrm{d}x\,. \tag{8}$$

Substituting from (2) and (4), the overlap integral yields

$$F = A_\mathrm{g}^2 A_\mathrm{r} A^2 \int_{-\infty}^{-h} \exp[2\gamma(x+h)] \times\left\{B\cos[\varrho(x+h)]+C\frac{\sigma}{\varrho}\sin[\varrho(x+h)]\right\}\mathrm{d}x \tag{9}$$

with $A = \cos(\kappa h)+(\delta/\kappa)\sin(\kappa h)$, $B = \cos(\sigma h)+(\Delta/\sigma)\times\sin(\sigma h)$, and $C = \sin(\sigma h)-(\Delta/\sigma)\cos(\sigma h)$. Hence, a simple integration gives

$$F = A_\mathrm{g}^2 A_\mathrm{r} A^2\left[\frac{2B\gamma - C\sigma}{4\gamma^2-\varrho^2}\right]. \tag{10}$$

The term $I_\mathrm{pm} = \sin^2(\Delta_\mathrm{pm}L/2)/(\Delta_\mathrm{pm}L/2)^2$ in (6), with $\Delta_\mathrm{pm} = 2\beta_\omega - \beta_{2\omega}$, describes the phase mismatch between all possible radiation modes and the guided pump mode. The overlap integral is a slowly varying function of ϱ comparing this mismatch factor and can be taken off the integration sign. If we consider relatively large Čerenkov angles (say $\theta > 2^\circ$), the integral in (6) may be approximately expressed in the form ($\varrho^2 = 4n_{\mathrm{s},2\omega}^2k^2 - \beta_{2\omega}^2 \rightarrow \mathrm{d}\varrho = \mathrm{d}\Delta_\mathrm{pm}\beta_{2\omega}/\varrho$) $\int_0^\infty I_\mathrm{pm}\,\mathrm{d}\varrho = \beta_{2\omega}\varrho^{-1}\int_{-\infty}^{\infty} I_\mathrm{pm}\,\mathrm{d}\Delta_\mathrm{pm} = 2\pi\beta_{2\omega}/(L\varrho)$. We express, according to Fig. 1, that $\cos\theta = \beta_{2\omega}/\varrho$. Hence,

$$P_{2\omega,C} = 2\pi\eta L P_\omega^2\cos\theta\,. \tag{11}$$

Note that the generated second-harmonic power is just proportional to the propagation length for large enough Čerenkov angles. However, the relation (11) diverges for small Čerenkov angles.

Assuming the case of the small Čerenkov angles, i.e. $\varrho \ll 1$, we may approximately express the mismatch factor as follows:

$$\Delta_\mathrm{pm} = 2\beta_\omega - \sqrt{4k^2n_{\mathrm{s},2\omega}^2 - \varrho^2} \approx 2\beta_\omega - 2kn_{\mathrm{s},2\omega} + \frac{\varrho^2}{4kn_{\mathrm{s},2\omega}}\,.$$

The integral in (6) then takes the form (we may again extend the integration interval, because of the sharply peaked behaviour of the 'sinc' function)

$$\int_{-\infty}^{\infty}\frac{\sin^2\left[\left(2\beta_\omega - 2kn_{\mathrm{s},2\omega}+\varrho^2/4kn_{\mathrm{s},2\omega}\right)L/2\right]}{\left[\left(2\beta_\omega - 2kn_{\mathrm{s},2\omega}+\varrho^2/4kn_{\mathrm{s},2\omega}\right)L/2\right]^2}\mathrm{d}\varrho \approx \frac{16}{3}\frac{\sqrt{2\pi kn_{\mathrm{s},2\omega}}}{\sqrt{L}}\,.$$

We have considered just the vicinity of well-phase-matched interaction, i.e. $\beta_\omega \cong kn_{\mathrm{s},2\omega}$. Substituting this result back into (6) yields the relation for the ČSHG for small Čerenkov angles close to the phase-matched interaction:

$$P_{2\omega,\mathrm{peak}} = \frac{8}{3}\sqrt{2\pi kn_{\mathrm{s},2\omega}}\eta P_\omega^2 L^{3/2}\,. \tag{12}$$

We have used the subscript peak because, as will be seen later, this relation is valid just in the peaked Čerenkov conversion efficiency (see Fig. 2). Here we find that the generated SH power follows $P_{2\omega} \propto L^{3/2}$. This result was first reported in [8] and may be further understood as a transition between the ČSHG and the classical guided–guided SHG interaction (GSHG) described e.g. in [9], where the generated SH power exhibits a quadratic dependence on the propagation length, as is well-known.

Let us further study the role of the overlap integral on the conversion-efficiency behaviour for small Čerenkov angles,

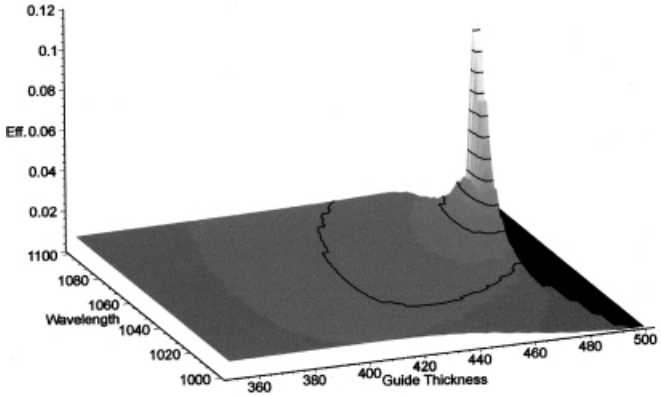

FIGURE 2 The conversion efficiency for a 1-mm-long KTP/Si_3N_4/SiO_2 device calculated by (11) and (12), respectively (Eff. $= P_{2\omega}/P_{\omega}^2$). ČSHG does not occur in the *dark area at the right corner* of the graph. The GSHG conversion efficiency would have been depicted there

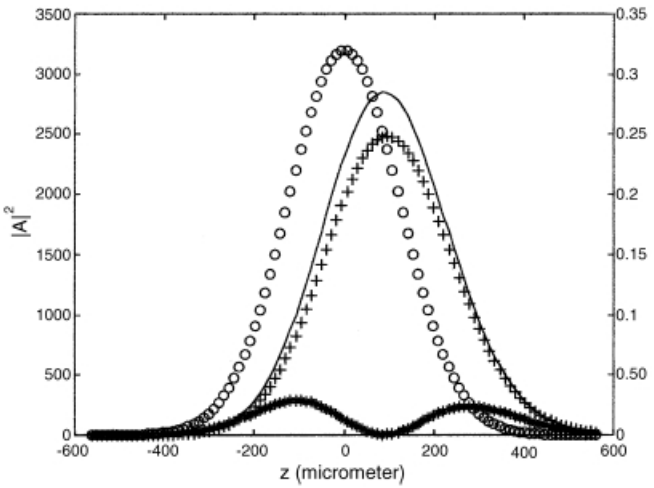

FIGURE 3 Power distribution related to the structure of Table 1. The incoming power ($\circ\circ\circ$), the reflected power ($+++$), and the transmitted power ($\star\star\star$) are given in W/m^2 (*left scale*); the modal power (*solid line*) is given in W/m (*right scale*). The total incoming power is 1 W/m

because the maximum of the conversion efficiency can be expected in this region. Since, as was said, $\varrho \to 0$ for $\theta \to 0°$, it can be seen from the normalisation constant of the radiation SH mode given in (5) that this constant is everywhere equal to zero for $\varrho = 0$ except for the very close vicinity given by the following relation:

$$\sigma \sin(\sigma h) = \Delta \cos(\sigma h) = 0 \tag{13}$$

which produces the modified dispersion relation giving the efficiency as follows (see also [10]):

$$\frac{\arctan(\delta/\kappa) + \arctan(\gamma/\kappa)}{\kappa} - \frac{\arctan(\Delta/\sigma) + \pi}{\sigma} = 0\,. \tag{14}$$

Solving the modified dispersion relation (14), one finds that there is only one suitable wavelength that can be converted with the highest conversion efficiency for given refractive indices. This can be done only for a particular thickness of the guiding layer, namely that given by the explicit expression $h = [\arctan(\delta/\kappa) + \arctan(\gamma/\kappa)]/\kappa$. Similar remarks hold for four-layer systems, which is the subject matter of our study (a grating may be understood as an extra layer of specific properties).

Finally, the peak exhibits a rather narrow FWHM (see Fig. 2) similar to the guided–guided SHG behaviour. In fact, this peak is the first point of the pure phase-matched SHG. This causes certain hurdles in device fabrication (e.g. an accuracy of the guide thickness of ± 0.2 nm is needed). These strict requirements are furthermore complicated with the demands necessary for an ordinary working ARM (see below). But, it still leads to a promising offer to exploit the Čerenkov regime apart from its peaked conversion efficiency, because of the 'automatically' satisfied phase matching.

The sharply peaked second-harmonic efficiency in the transition point was experimentally studied in two papers by Doumuki et al. [2, 3]. We recognised [8, Fig. 7b] and further considered [10, (7)] that the generated SH power in the position of the peaked ČSHG conversion efficiency obeys approximately (please note the difference of the factor of two missed in [8, 10]):

$$P_{2\omega,\mathrm{peak}} \approx 0.12 \left(\frac{L}{L_{1\,\mathrm{mm}}} \right)^{3/2} P_{\omega}^2\,, \tag{15}$$

Layer	Thickness/nm	n(1053 nm)	n(526.5 nm)
Air	–	1	1
Grating	180	1.5607	1.5849
Si_3N_4	462	1.9676	2.006
KTP	–	1.83005	1.889

TABLE 1 Relevant parameters for the structure used for ČSHG; the grating period was 440 nm and a duty cycle of 0.5 was assumed

where the bracketed term denotes the relative interaction length related to 1 mm. The pump power in the relation (15) is understood to be normalised to 1 μm of the slab width.

3 The ARM structure

Si_3N_4 layers were deposited by PECVD (plasma-enhanced chemical vapour deposition) on a KTP substrate. The gratings were made by standard holographic exposure (with an Ar laser) of a resist, followed by developing and ion-beam etching for the transfer of the grating from the resist film into the Si_3N_4 layer. The parameters of the fabricated structure are given by Table 1; the KTP substrate was oriented such that all electrical vectors are along the z-axis. The calculations based on [11] have led to the following quantities: propagation constant $\beta = 11.177\ /\mu\mathrm{m}$, coupling constant $\kappa = 0.0090\ /\mu\mathrm{m}$, and angle of excitation for maximum reflection 31.33 degrees.

The structure was excited by a beam with a width of $2w = 500\,\mu\mathrm{m}$. The amplitude distributions, calculated using the analytical expressions of [11], assuming 1 W/m incoming power, are given in Fig. 3. From these we find for the angle corresponding to maximum reflection a theoretical power reflection of 87.5%, and a power transmission of 12.5%. Using standard theory for ČSHG (see e.g. [8] and references therein) we found, based on a value of $\chi^{(2)}_{zzz} = 23.6$ pm/V, a conversion efficiency of $\eta = 4.0 \times 10^{-6}\ /\mathrm{W}$. Using the latter and the calculated modal amplitude distribution, a SH power not higher than $\approx 0.4\,\mu\mathrm{W}$ was calculated.

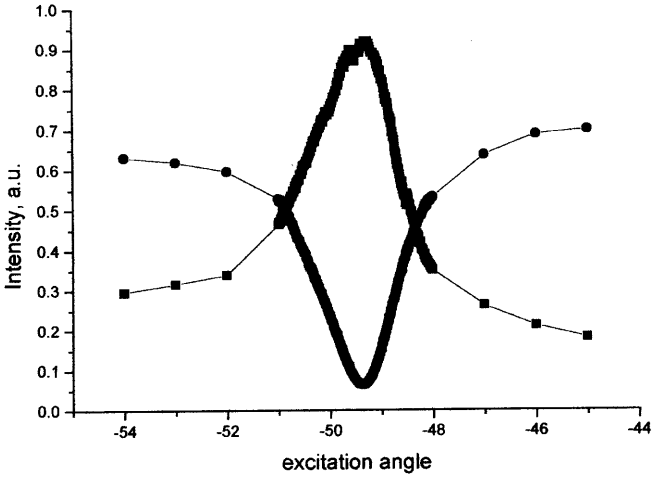

FIGURE 4 Experimental power reflection (peaked curve) and transmission curves for linear ARM (corrugated Si_3N_4 layer on the glass substrate). Total Si_3N_4 layer thickness is 506.6 nm. 200 nm of this layer is corrugated with corrugation period 460 nm

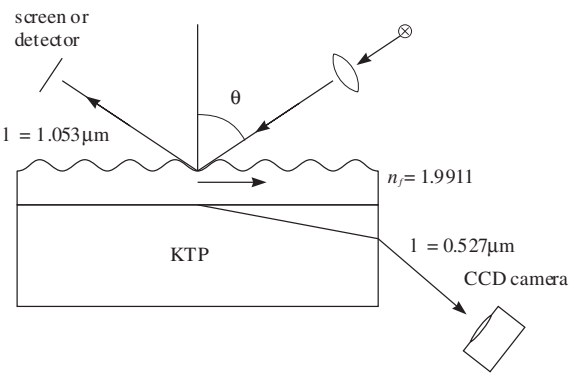

FIGURE 5 The scheme of the experimental set-up for ČSHG

4 Experiments

As a first step we measured the transmission and reflection of the structure for low power levels. With the same experimental parameters as above we found the curves as presented in Fig. 4 for a linear ARM structure. The minimum transmission is of the correct order of magnitude ($\sim 4\%$ of the total power) but the peak in the reflection is less than expected ($\sim 92\%$), attributed to scattering due to imperfections, which becomes relatively large when the guided mode is resonantly excited.

At a power level of 2 W of the fundamental beam, ČSHG could be observed in the form of green light escaping through the KTP substrate. A green power level of $\approx 1\,\mu$W was measured, in close agreement with the theoretical value (the scheme of the experimental set-up is presented in Fig. 5).

5 Why is an ARM necessary for ČSHG?

The next question is: why need we use ARM structures for ČSHG experiments? Can this approach give us some advantages? Let us consider some experimental schemes where the use of an ARM could be useful for ČSHG experiments. Figure 6 presents the scheme where an ARM structure is used with an additional mirror. Calculations show

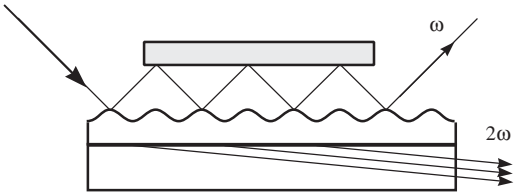

FIGURE 6 Combination of ARM and flat mirror

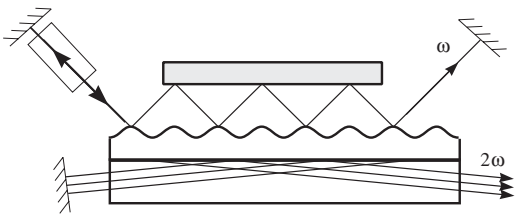

FIGURE 7 Combined ARM structure placed inside a laser cavity

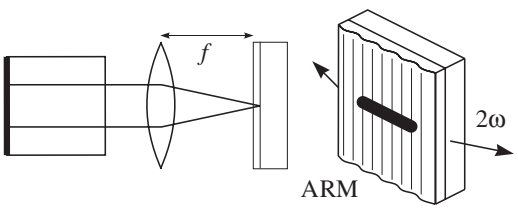

FIGURE 8 ARM structure used as a mirror in a Fabry–Pérot cavity together with a cylindrical lens

that a combination of an abnormal reflection mirror with the usual mirror gives a sufficient increase of the SH signal.

Figure 7 presents the scheme of a laser cavity with an ARM and an additional mirror inside it. In this scheme we can keep all energy inside the cavity and as a consequence we can increase the power density inside the optical waveguide. In both cases the type of laser we used in our experiments is not important. However, it is necessary to note that use of an ARM structure inside a solid-state laser cavity is not effective. Our experiments with an ARM inside a solid-state laser cavity (in collaboration with the research group of Dr. V.I. Ustyugov, Institute of Laser Physics, St. Petersburg) showed that total losses equal to 8% (see Fig. 4) could not allow us to obtain an effective device. For this reason we believe that the better solution is to use an ARM structure inside the cavity of a semiconductor laser. The last results demonstrated that ARM structures could be used effectively inside the cavity of a semiconductor laser [12, 13].

Figure 8 presents the scheme of using an ARM inside a semiconductor laser cavity for ČSHG. We believe that this scheme can serve as a prototype of a device for a direct frequency-doubling device, instead of frequency doubling as an alternative to intra-cavity frequency doubling in a solid-state laser with pumping by a semiconductor laser.

6 Conclusions

The presented study investigated an interesting connection of two phenomena. Namely, an ARM structure, which allows for wavelength selectivity and wavelength tuning, combined with SHG in one device. Both phenomena have already been studied separately in detail. Exploitation of both

phenomena simultaneously offers several new experimental possibilities. But, as can be concluded from the presented study, obtaining efficient SHG needs special care. The efficiency might be increased in the first place by using the ARM-SHG device in a laser cavity with high intra-cavity power. Secondly, the interaction length in the presented device is only a few hundreds of micrometres, and as the efficiency in the Čerenkov regime (not too close to the high-efficiency peaks) is proportional to the length, the efficiency can be further increased by using lasers with a broader (along the propagation direction) beam, together with a correspondingly weaker grating. An even further increase of efficiency can be obtained by frequency conversion close to the high-efficiency peaks in the Čerenkov regime, or on the high-efficiency line in the guided–guided SHG regime, by utilising e.g. quasi-phase matching.

ACKNOWLEDGEMENTS This work was supported by EC Inco-Copernicus 960194 and NWO 047.006.014 Projects.

REFERENCES

1 H. Tamada: IEEE J. Quantum Electron. **QE-27**, 502 (1991)
2 T. Doumuki, H. Tamada, M. Saitoh: Appl. Phys. Lett. **64**, 3533 (1994)
3 T. Doumuki, H. Tamada, M. Saitoh: Appl. Phys. Lett. **65**, 2519 (1994)
4 N. Asai, H. Tamada, I. Fujiwara, J. Seto: J. Appl. Phys. **72**, 4521 (1992)
5 R.-S. Chang, S.-Y. Shaw: J. Mod. Opt. **45**, 103 (1998)
6 L. Kotačka, J. Čtyroký, H.J.W.M. Hoekstra: in OSA Tech. Dig. – NLGW'99 (OSA, Washington, DC 1999) p. 380
7 D. Marcuse: Theory of Dielectric Optical Waveguides (Academic, New York, London 1974)
8 J. Čtyroký, L. Kotačka: Opt. Quantum Electron. **32**, 799 (2000)
9 A. Yariv: IEEE J. Quantum Electron. **QE-9**, 919 (1973)
10 L. Kotačka, J. Čtyroký, H.J.W.M. Hoekstra: Acta Phys. Pol. A **99**, 135 (2001)
11 H.J.W.M. Hoekstra: Opt. Quantum Electron. **32**, 735 (2000)
12 N.V. Baidus, I.F. Salakhutdinov, H.J.W.M. Hoekstra, B.N. Zvonkov, S.M. Nekorkin, V.A. Sychugov: Photon. Technol. Lett. (2001) to be published
13 G. Levy-Yurista, A.A. Friesem, E. Pawlowski, L. Kuller, R. Ludwig, H.G. Weber, A. Donval, E. Toussaere, J. Zyss: Opt. Mater. **17**, 149 (2001)